Genetic bases of resistance to the rice *hoja blanca* disease deciphered by a QTL approach

Alexander Silva[1], María Elker Montoya[2], Constanza Quintero[1], Juan Cuasquer[1], Joe Tohme[1], Eduardo Graterol[2], Maribel Cruz[2,*], Mathias Lorieux[1,3,*]

[1]Alliance Bioversity-CIAT, Cali, Colombia
[2]FLAR-Fondo Latinoamericano para Arroz de Riego, Cali, Colombia
[3]DIADE, University of Montpellier, Cirad, IRD, Montpellier, France
[*]Corresponding authors: mathias.lorieux@ird.fr and maribel.cruz@cgiar.org

ABSTRACT

Rice *hoja blanca* (RHB) is one of the most serious diseases in rice growing areas in tropical Americas. Its causal agent is *Rice hoja blanca virus* (RHBV), transmitted by the planthopper *Tagosodes orizicolus* Müir. Genetic resistance is the most effective and environment-friendly way of controlling the disease. So far, only one major quantitative trait locus (QTL) of *Oryza sativa* ssp. *japonica* origin, *qHBV4.1*, that alters incidence of the virus symptoms in two Colombian cultivars has been reported. This resistance has already started to be broken, stressing the urgent need for diversifying the resistance sources. In the present study we performed a search for new QTLs of *O. sativa indica* origin associated with RHB resistance. We used four $F_{2:3}$ segregating populations derived from *indica* resistant varieties crossed with a highly susceptible *japonica* pivot parent. Beside the standard method for measuring disease incidence, we developed a new method based on computer-assisted image processing to determine the affected leaf area (ALA) as a measure of symptom severity. Based on the disease severity and incidence scores in the F_3 families under greenhouse conditions, and SNP genotyping of the F_2 individuals, we identified four new *indica* QTLs for RHB resistance on rice chromosomes 4, 6 and 11, namely $qHBV4.2^{WAS208}$, $qHBV6.1^{PTB25}$, *qHBV11.1* and *qHBV11.2*. We also confirmed the wide-range action of *qHBV4.1*. Among the five QTLs, *qHBV4.1* and *qHBV11.1* had the largest effects on incidence and severity, respectively. These results provide a more complete understanding of the genetic bases of RHBV resistance in the cultivated rice gene pool, and can be used to develop marker-aided breeding strategies to improve RHB resistance. The power of joint- and meta- analyses allowed precise mapping and candidate gene identification, providing the basis for positional cloning of the two major QTLs *qHBV4.1* and *qHBV11.1*.

KEY WORDS

Rice hoja blanca virus (RHBV), Rice *hoja blanca* disease (RHB), Quantitative trait locus (QTL), candidate gene

INTRODUCTION

The rice *hoja blanca* (RHB) disease is one of the most important constraints to rice productivity in the tropical zone of Americas, causing yield losses in many countries, including Colombia,

Costa Rica, Ecuador, Guyana, Panama, Peru, Dominican Republic, Nicaragua and Venezuela (Morales and Jennings 2010). Its causal agent is the *Rice hoja blanca virus* (RHBV), a *Tenuivirus* transmitted by the planthopper *Tagosodes orizicolus* M. (Hemiptera:Delphacidae). Genetic resistance to both the virus and its vector insect is key for a successful, environment- and consumers health-friendly, integrated crop management. No real immunity has been found in the cultivated rice germplasm, and even in resistant materials, the plantlets (< 10 days old) can show susceptibility to the virus. Nonetheless, a handful of varieties – including the two Colombian cultivars, Fedearroz 50 and Fedearroz 2000 – with good resistance level have been bred in the past and have been important to stabilize rice production. Fedearroz 2000 is still the most resistant commercial variety, however, the incidence of the disease has increased under field and controlled conditions. Fedearroz 50 has turned virus-susceptible in the past years in the field, probably due to virus mutations that allowed it to overcome the resistance. Thus, there is an urgent need for diversifying the sources of genetic resistance in order to breed new varieties with more durable resistance. Genetic resistance to RHB disease can be decomposed into resistance to the virus itself, and resistance to its insect vector.

In a previous study, we reported a major QTL on the short arm of chromosome 4 for resistance to RHBV, shared by Fedearroz 50 and Fedearroz 2000, abbreviated as FD 50 and FD 2000 in this paper (Romero et al. 2014). This QTL, called here *qHBV4.1*, controlled RHB *incidence*, measured as the percentage of plants that show symptoms of the viral infection, no matter the level of the symptoms. Incidence is of course an important parameter of the epidemics of a disease. Yet, its *severity* is certainly as much as important: if severity is low, a high incidence might have no significant impact on plant viability, panicle development, or grain yield. Additional to RHBV incidence, we thus designed – and report in this study – new experiments to decipher the genetic control of RHB resistance seen as symptoms severity, measured by computer-aided image processing of the affected leaf area (ALA).

The *Oryza sativa* species is divided into two main clades, *indica* and *japonica*, which can be considered as sub-species. The *indica* and *japonica* are themselves divided into 15 subgroups (Li et al. 2014). Using genomic sequencing data, it is possible to infer the *indica* or *japonica* origin of an accession at a particular chromosome location by local ancestry analysis (Santos et al. 2019). We showed by local ancestry analysis showed that, although FD 50 and FD 2000 are mostly of *indica* genetic background, *qHBV4.1* in those two cultivars was found to be of *japonica* origin and was surrounded by several hundred kilobase pairs of *japonica* DNA. We found desirable to search for *indica* resistance QTLs in order to ensure better compatibility with tropical irrigated materials in breeding programs, and also to increase the diversity of the available sources of genetic resistance. Based on the encouraging screening work by the FLAR (Fondo Latinoamericano para Arroz de Riego) team (Cruz-Gallego et al. 2018), we thus designed a new QTL analysis based on four crosses involving new resistance sources.

74 ## MATERIALS AND METHODS

75 ### Plant materials

76 Four *O. sativa* ssp. *indica* accessions were selected amongst the most resistant materials
77 identified in (Cruz-Gallego et al. 2018): WAS 208-B-B-5-1-1-3 (IRGC 121855) thereafter
78 abbreviated as WAS 208), Badkalamkati (IRGC 45011) (abb. Badka), PTB 25 (IRGC 6386) and
79 Fedearroz 2000 (IRGC 124388) (abb. FD 2000). The main selection criteria were (1) selected
80 sources should show consistent and high resistance to RHB and (2) they should cover the
81 genetic diversity spectrum of the *indica* cluster. Then, the four resistance sources were crossed
82 with the highly susceptible *japonica* line Bluebonnet 50 (IRGC 121874) (abb. BBT 50), using
83 BBT 50 as the male parent. Candidate F_1 hybrids were checked for self-pollination of the mother
84 plant with 48 SNP (single nucleotide polymorphism) markers distributed along the rice
85 genome. F_2 (S_1) populations were derived from self-pollination of the verified F_1 hybrids. Each
86 F_2 plant was self-pollinated to produce F_3 (S_2) families. All panicles involved in crosses or self-
87 pollination were bagged to avoid out-crossing.

88 ### Population sizes

89 The following population sizes were used for both genotyping in F_2 plants and trait scoring in
90 F_3 families: WAS 208 × BBT 50: 104 F_2, 1,040 F_3 (ALA), 6,240 F_3 (incidence); Badka × BBT 50:
91 105 F_2, 1,050 F_3 (ALA), 6,300 F_3 (incidence); PTB 25 × BBT 50: 108 F_2, 1,080 F_3, 6,480
92 (incidence); FD 2000 × BBT 50: 105 F_2, 1,050 F_3 (ALA), 6,300 F_3 (incidence). Populations sizes
93 for ALA scoring are significantly lower than for incidence, however, as ALA is assessed using
94 tube-based phenotyping (non-choice feeding test), precision is higher than for incidence
95 measured in trays (see hereby).

96 ### Evaluation of RHB resistance

97 To evaluate the level of resistance – or susceptibility – of the F_3 plants, we looked at two
98 complementary aspects of the disease: the *incidence* and the *severity* of the symptoms. *Incidence*
99 is simply defined by the proportion of diseased plants in a population, while *severity* is the area
100 or volume of plant tissue that is visibly diseased (Campbell and Neher 1994). The F_3 families,
101 parents and check lines were evaluated under greenhouse conditions, at the CIAT (Centro
102 Internacional de Agricultura Tropical, International Centre for Tropical Agriculture)
103 headquarters in Palmira, Colombia.

104 #### *Virulent insect colonies*

105 *T. orizicolus* virulent insects were obtained from colonies maintained at CIAT. The RHBV-
106 harboring colony contained insects that were fed on RHBV-infected plants and allowed to
107 reproduce on BBT 50. To determine the percentage of virulent insects in this colony, 200
108 individual nymphs were tested for virulence on separate, caged, RHB-susceptible 8-day-old
109 seedlings.

110 #### *Incidence*

Here we consider incidence as the percentage of plants showing any level of RHB symptoms. We consider the absence of symptoms as a sign of absence of infection, not as extreme tolerance. F_3 materials and controls were planted in plastic trays containing 17 furrows of 20 plants each. Each tray contained a furrow of each parent – BBT 50 also served as a susceptible control – and the controls FD 2000 (resistant) and Colombia 1 (intermediate). The trays were placed in a mesh cage 18 days after sowing, and infested by mass release of *T. orizicolus* with virulence between 50% and 65%, with an average of four nymphs per plant. The nymphs were allowed to feed for three days on the plants, after which they were eliminated with water rinsing. A randomized complete block design was used with three replicates (20 plants from each F_3 family per replicate), where each block represented a cage. Incidence assessment was made 35 days after infestation (DAI) by counting the plants showing disease symptoms, per row.

Severity

In order to test the severity of RHB, 10 plants per F_3 family were measured individually. 18 days after sowing, plants were transferred in individual transparent tubes with 3 nymphs per plant. Nymphs were allowed to feed for three days on the plants. Symptoms severity was measured using a novel methodology based on computer-assisted image processing. Briefly, images of the three youngest leaves infected plants were taken using a reference scale (a ruler) and a contrasting background under homogeneous light exposure. Raw images of plants with symptoms (Figure 1A) were processed using the ImageJ software (https://imagej.nih.gov/ij) in two steps: in the first step, brightness was decreased to eliminate the areas affected by the disease (Figure 1B). Then, the image was binarized, *i.e.*, converted to black and white (Figure 1C). The number of black pixels was thus representing the healthy area H of the leaf, according to the previously calibrated reference scale. In the second step, a binarization process allowed to calculate the total area T (Figure 1D). The affected leaf area (ALA) by the virus was then calculated in each F_3 plant as:

$$ALA = \begin{cases} (T - H)/T \;\; for\ plants\ showing\ symptoms \\ \quad 0\ for\ plants\ with\ no\ symptoms \end{cases}$$

The ALA of each F_3 family was then calculated as the average of the ALA values of the 10 F_3 plants. In an attempt to remove possible correlation effects with incidence, we also calculated the averaged ALA only over the plants that showed symptoms (ALA_strict).

Statistical treatment

Since ALA was measured as the ratio of affected/total leaf area for each family in each block, a weighted ALA was calculated with a generalized linear mixed model (MLGM) using the gamma distribution. The incidence variable was analyzed with an MLGM using the binomial distribution. The MLGM procedure is used for variables that are not necessarily normally distributed. For each variable, an analysis of variance was performed to test for differences between families and to evaluate the effect of the blocks. Subsequently, adjusted means were calculated for each family and a mean comparison test (t-test) was performed to identify those families that were more resistant or equal to the resistant parent. The descriptive analysis was

150 performed in the R program and the other analyses were performed in the SAS® statistical
151 program.

152 **SNP marker development**

153 Whole-genome sequences (WGS) of parental lines, available from previous studies (Li et al.
154 2014; Duitama et al. 2015; Cruz-Gallego et al. 2018) and the IRGSP 1.0 Nipponbare reference
155 genome were compared *in silico* using the Next Generation Sequencing Eclipse Plugin, NGSEP
156 (Duitama et al. 2014). Variant detection and annotation were performed with NGSEP and SNP
157 positions were determined relative to the reference genome. Informative biallelic SNPs were
158 filtered based on the following characteristics of their flanking sequence: minimum 30 bp
159 between the target SNP and other variant and GC content between 20 and 65%. The flanking
160 sequence of 100bp upstream and downstream the target SNP was retrieved and submitted to
161 D3 assay design web-based tool (https://d3.fluidigm.com) to develop Fluidigm® SNPtype
162 assays. SNPs were chosen based on their design quality score and their genomic position.

163 **DNA extraction**

164 Leaf tissue was collected from 15-days-old F_2 plants. Samples were frozen in liquid nitrogen and
165 stored at –80°C until processed. Plant DNA was isolated in 96-racked tubes using a modified
166 version of a method previously described (Risterucci et al. 2000) as follows: 480 µl of extraction
167 buffer was added to 150 mg of ground frozen leaf tissue. The buffer was 100 mM Tris (pH =
168 8.0), 2M NaCl, 20 mM EDTA (pH = 8.0), 2% MATAB, 0.5% sodium bisulfite, and 1% PEG 8000.
169 This mixture was homogenized and incubated in a water bath at 74°C for 30 min. Subsequently,
170 480 µl of chloroform:isoamyl-alcohol (24:1) was added and the mixture was centrifuged at
171 3000 rpm in a Sorvall® centrifuge with a GLA-3000 rotor. Supernatants were precipitated with
172 270 µl of isopropanol at –20°C for one hour and centrifuged at 3000 rpm. The pellets were
173 washed with 200 µl of 80% ethanol and allowed to dry at 40°C by inverting the tubes for one
174 hour. DNA was resuspended in Tris-EDTA [10 mM Tris-HCl, pH8 and 1 mM EDTA, pH8)
175 containing 40µg/ml of RNAse A and spectrophotometric quantification was done using a
176 multimode plate reader Synergy H1 (Biotek®). DNAs were normalized at 60ng/µl for
177 subsequent processing.

178 **Genotype scoring**

179 F_2 individuals and parents were scored for polymorphic SNPs in each population using the
180 Fluidigm® nanofluidic genotyping platform, according to the manufacturer's protocols. Briefly,
181 pre-amplification of targets regions was done in a 5µl multiplex-PCR mixture. The amplicons
182 were used as template for allele specific-PCR that was conducted in 48 × 48 integrated fluidic
183 circuit (IFCs) of the Fluidigm® genotyping platform. Fluorescent images of the IFCs were
184 acquired in an EP1 reader and analyzed with the Fluidigm® Genotyping Analysis Software.

185 **Linkage maps construction**

186 Genetic maps were calculated with MapDisto 2.0 (Lorieux 2012; Heffelfinger et al. 2017)
187 (http://mapdisto.free.fr). Goodness-of-fit to Mendelian segregation (1:2:1) was tested for each
188 marker by computing the chi-squared (χ^2) statistic with the 'Segregation χ^2s' function. As the

189 SNP markers were defined from WGS, we kept their order on the physical map or rice. For each
190 cross separately, we checked the data for singletons (e.g., the "B" in "AAAAAAA**B**AAAAAA" is a
191 singleton) with the 'Replace errors by flanking genotypes' function, with a maximum
192 probability of a singleton to occur of 0.001. A few missing data were inferred using the 'Replace
193 missing data by flanking genotypes' function, with the same threshold. Recombination fractions
194 were calculated with the standard EM algorithm (appendix 1 in Lorieux 2021) converted to
195 centimorgans (cM) with the Kosambi mapping function (Kosambi 1944).

196 **QTL mapping**

197 Data files were prepared using the 'Export map and data' function of MapDisto 2.0. Analyses of
198 distribution of the phenotypic traits as well as QTL detection were performed using the Qgene
199 4.0 program (Joehanes and Nelson 2008) (http://www.qgene.org). For QTL detection, the LOD
200 score statistics were calculated with different methods and then compared: single-marker
201 regression (SMR), simple interval mapping (SIM) and composite interval mapping (CIM). The
202 forward cofactor selection option was used in CIM. Additivity and dominance effects were
203 calculated according to Falconer (1960). Empirical thresholds to declare the presence of a QTL
204 were obtained using the resampling by permutation method, performing 10,000 (SMR) or
205 1,000 (CIM) iterations for each trait-chromosome combination. In order to correct for possible
206 erroneous phenotypic data corresponding to escape, mis-scoring, or incomplete penetrance, all
207 positive QTLs were additionally confirmed by analysis of outliers in the trait distribution using
208 the 'Plot trait vs. genotype' module of MapDisto. This module allows to calculate corrected
209 single-marker regression F-test values after detecting and removing outlier data in each marker
210 genotypic sub-class.

211 In the case of a secondary LOD score peak linked to a major peak of a QTL, in order to determine
212 if the secondary peak corresponded to a true QTL or to an artifact – or "fake QTL" – a detailed
213 analysis of the distribution of recombination fractions along the chromosome was performed,
214 following the method of Lorieux (2018). The analysis looked for restriction of recombination
215 fractions that could induce artificial linkage disequilibrium between the major and the
216 secondary LOD score peaks. If artificial linkage disequilibrium was detected, then the secondary
217 peak was declared an artifact. Interaction or epistasis was tested using the R/qtl 'scantwo'
218 function (Prins et al. 2010).

219 When a QTL is found in more than one cross, a joint or a meta-analysis can increase the
220 precision of the QTL location. A joint analysis is considering several populations as one single
221 population, and thus necessitates (1) harmonizing the genotypic and phenotypic data among
222 the populations, then (2) merging the genotypic and phenotypic data into joint matrices, and
223 (3) running the QTL analysis on the joint dataset. On the contrary, in the meta-analysis, a QTL
224 analysis is firstly performed in each population separately, then the resulting scores are
225 combined using the Fisher's method (Fisher 1932).

226 To harmonize the genotypic data, as different markers segregated in the four populations, we
227 created a genotype matrix from the union of the four individual data sets. Markers with no data
228 in some of the populations were imputed using the R/qtl 'Argmax' function. For joint analysis,

229 only the populations that showed a QTL in single-population analyses were pooled. Meta-
230 analysis was always ran using the four populations pooled.

231 The phenotypic data were harmonized using centralized and normalized phenotypic data, that
232 is

233 $$P_M0_V1_i = (P_i - M)/S$$

234 Where P_i is the phenotypic value of the individual i, M is the average value in the population,
235 and S is the standard deviation in the population. Centralized and normalized data always have
236 a mean equal to 0 and a variance equal to 1, making them more suitable for combination in joint
237 analyses.

238 Both joint- and meta-QTL analyses were run using MapDisto 2.0.

239 To identify candidate genes in the fine-mapped regions, the MSU Rice genome annotation
240 database and the Overview of Functionally Characterized Genes in Rice Online database
241 (OGRO) (Yamamoto et al. 2012) were used. A 1-LOD drop-off support interval was used to
242 define the search region for each QTL.

243 RESULTS

244 SNP markers and genetic maps

245 A total of 332 SNPs were identified as segregating in at least one of the four crosses. Table S1
246 summarizes the main characteristics of each SNP: position on the genome, allele in the RefSeq
247 and the susceptible and resistant parents, and 250 bp flanking sequences (left and right).

248 Table 1 summarizes the main statistics of the individual genetic maps obtained for each cross.
249 Overall, we obtained genetic map sizes coherent with their expected size according to ten high-
250 quality maps based on flexible and scalable genotyping by sequencing (fsGBS) (Heffelfinger et
251 al. 2014; Fragoso et al. 2017), the absence of pollen contamination in the self-pollination
252 process and the high quality of the SNP data.

253 ***Segregation distortion (SD):*** SD was observed on chromosome 3 (11.1-21.0 Mbp) in the
254 crosses involving WAS 208, Badka and FD 2000. This region is commonly affected by SD in
255 *indica* × *japonica* crosses (Wang et al. 2009; Fragoso et al. 2017). The homozygotes for the
256 donor allele (AA genotype) were favored over both the homozygotes for the susceptible parent
257 allele (BB genotype) and the heterozygotes (AB) (Figure S1). In the cross WAS 208 × BBT 50
258 cross, a pattern of SD was also observed on chromosome 8 (3.53-16.44 Mbp), where the AB
259 genotypes were favored over the AA. In the cross PTB 25 × BBT 50, segregation distortion was
260 observed on chromosomes 2 (20.1 Mbp, 47AA:50AB:11BB), 6 (2.9-7.9 Mbp, 34AA:64AB:10BB)
261 and 9 (10.8-12.2 Mbp, 42AA:54AB:12BB).

262 **RHB incidence and severity variation**

263 In the cross WAS 208 × BBT 50, the parental lines showed 24.2±11.9% and 98.1±3.2% of RHB
264 incidence and 25.8±32.7% and 69.5±37.7% of RHB severity in WAS 208 and BBT 50,
265 respectively. The F_3 families (each representing one F_2 parental plant) exhibited a continuous
266 variation of incidence ranged between 21.4% and 100%, as well as a variation of severity
267 ranged between 9% and 68% (Figure 2). The high incidence score for the susceptible parent
268 BBT 50 – almost 100% – and the maximum values in the F_3 families indicate a perfect infection
269 efficiency. The similarity between the severity score for BBT 50 and the maximum scores in F_3
270 families indicates that the experimental design, and in particular the population size, were
271 adequate to capture the range of variation between the parental values.

272 In the cross Badka × BBT 50, the resistant and susceptible parents exhibited 32.8±12.4% and
273 98.9±2.9% of RHB incidence, respectively. In the same order, these parents displayed
274 35.3±17% and 81.6±27.7% of severity. The incidence in the F_3 families ranged between 13%
275 to 98%, and the severity varied between 11% and 80% (Figure 2). A positive correlation
276 between incidence and severity of the disease was detected (r=0.56, p<0.0001) using the entire
277 population, suggesting a common partial genetic control for both assessments of RHB disease.
278 Some F_3 families exhibited lower incidence and severity than the resistant parent Badka.

279 In the cross PTB 25 x BBT 50, the incidence of the resistant and susceptible parents was
280 3.4±3.5% and 98.2±3.3%, respectively, and ranged between 5% to 96% in the F_3 families.
281 Furthermore, PTB 25 and BBT 50 showed 11.8±22.1% and 68.1±25.1% of severity,
282 respectively. The same trait varied between 7% and 69% in the F_3 families.

283 In the cross FD 2000 × BBT 50, the resistant and susceptible parents showed 20.8±8.8% and
284 75.4±14.1% of RHB incidence, and 3.4±6.5% and 50.1±33.1% of severity, respectively. In the F_3
285 families; incidence ranged between 10% and 90%, and severity between 0% and 59%. The
286 incidence and severity for the susceptible parent BBT 50 were notably lower than in the crosses
287 before mentioned, indicating a low infection efficiency that can affect the power of QTL
288 detection and the QTL effects estimation. In contrast, the incidence of FD 2000 was higher than
289 in previous works (Romero et al. 2014; Cruz-Gallego et al. 2018).

290 Incidence and severity showed correlation between 0.42 and 0.66 (Table 2), indicating either a
291 common genetic control of the two traits, or that they are interdependent.

292 **The major QTL *qHBV4.1* for RHBV incidence is present in most donors**

293 A major QTL, *qHBV4.1,* on chromosome 4 for RHBV incidence was identified by SMR, SIM and
294 CIM in the crosses Badka × BBT 50 (LOD=20.97, R^2=0.63), PTB 25 × BBT 50 (LOD=21.26,
295 R^2=0.60) and FD 2000 × BBT 50 (LOD=9.11, R^2=0.34) (Table 3). It was not detected in the cross
296 WAS 208 × BBT 50, although a fake QTL analysis (Lorieux 2018) showed that it could be
297 present in WAS 208, but with a much smaller effect (data not shown). The QTL support
298 intervals are overlapping in the three populations, suggesting that the same QTL is shared by
299 the three resistance donors. Joint analysis gave a LOD=47.00 and R^2=0.42 at the position ~3.56
300 Mbp. The *qHBV4.1* position also corresponds to a previously identified locus characterized as

301 the major contributor to RHBV resistance in FD 2000 and FD 50 (Romero *et al.*, 2014),
302 confirming the wide range of action of this QTL. It explained 34-63% of the trait variance,
303 indicating that *qHBV4.1* is a major regulating factor of incidence of RHBV infection. The
304 estimation of QTL effects for *qHBV4.1* showed that this QTL is mostly of the additive type. The
305 same genomic region was also associated with RHB severity in the same crosses, however with
306 lower LOD scores and R^2 values (LOD=6.69-8.50, R^2=25-31%).

307 **A new major QTL for RHB incidence, *qHBV4.2*, identified in WAS 208**

308 The control of RHB incidence in WAS 208 was mainly explained by a different QTL on
309 chromosome 4, designated as $qHBV4.2^{WAS208}$ (LOD=15.49, R^2=0.52) by SMR, SIM and CIM. This
310 QTL was not found in the other crosses (Table 3). This newly discovered QTL was located
311 between 21.29 and 21.81 Mbp and explained 52% of the incidence variance. *qHBV4.2* is
312 therefore another major QTL for RHB incidence that seems less frequent than *qHBV4.1* in the
313 rice germplasm.

314 **Two new QTLs for RHB incidence identified in WAS 208 and PTB 25**

315 Two additional QTLs, although of lesser effect, were detected for RHB incidence (Table 4):

316 – $qHBV6.1^{PTB25}$ on chromosome 6 (0.18-1.76 Mbp, LOD_{SIM}=3.64, LOD_{CIM}=9.71, R^2=25%), mostly
317 of the additive type effect and detected in the PTB 25 × BBT 50 cross only.

318 – *qHBV11.2* on chromosome 11 in the crosses involving WAS 208 (7.43-11.9 Mbp, LOD_{CIM}=5.02,
319 R^2=21%) and PTB 25 (7.43-16.6 Mbp, LOD_{CIM}=5.9, R^2=24.2%). However, the SMR or SIM
320 methods produced LOD scores under the retained threshold (Tables 3 and 5).

321 **A new QTL, *qHBV11.1*, controls RHB severity**

322 One of the most interesting results of this work is the discovery of a new QTL associated with
323 RHB symptoms severity (measured as ALA). It was detected on chromosome 11 in the crosses
324 WAS 208 × BBT 50 (18.0-18.8 Mbp, LOD=5.32, R^2=0.21), Badka × BBT 50 (17.8-18.5 Mbp,
325 LOD=4.68, R^2=0.19) and FD 2000 × BBT 50 (17.8-18.5 Mbp, LOD=8.98, R^2=0.33). This QTL was
326 designated as *qHBV11.1* and explained 17-33% (SIM) or 19-37% (CIM) of the trait variation,
327 depending on the cross (Tables 3 and 4). The QTL effects in the populations involving WAS 208
328 and Badka indicate an additive behavior of *qHBV11.1*, while in FD 2000 × BBT 50 it seems to be
329 more dominant (Table 3). In the cross FD 2000 × BBT 50, *qHBV11.1* was also significant for RHB
330 incidence, although with lower statistics (LOD=7.43, R^2=0.29). Interestingly, *qHBV11.1* was
331 significant for ALA_strict (LOD=4.05), which suggests that two distinct genes act onto RHB
332 severity, possibly in interaction.

333 **The *qHBV4.1* and *qHBV11.1* QTLs show strong interaction**

334 Testing interaction between QTL regions with the R/qtl "scantwo" function produced a strong
335 signal between the two QTLs *qHBV4.1* and *qHBV11.1* (LOD>15) (see example for the
336 FD 2000 × BBT 50 cross in Figure S2), revealing either an epistasis relationship between the
337 two regions, or a simple interdependency between the two traits. This is coherent with the
338 positive correlation observed between severity and incidence.

339 **Joint- and meta-analyses provide good candidates for QTL cloning**

340 The joint and meta-analyses approaches allow pooling populations, providing more resolution
341 for QTL mapping. This allowed us identifying candidate genes that could underlie two of the
342 QTLs we discovered.

343 ***The qHBV4.1 region contains the AGO-4 Argonaute gene***

344 In the *qHBV4.1* region, 33 genes encoding proteins with unknown function, five hypothetical
345 genes, four genes encoding different types of kinases, two genes of the MEG (maternally
346 expressed gene) family involved in the translocation of nutrients to the seed, and one *Argonaute*
347 gene were identified. The most interesting gene within the *qHBV4.1* region is probably the
348 *Argonaute* AGO-4 (MSU: LOC_Os04g06770, Chr4:3,562,793-3,555,220bp). AGO proteins are
349 effector proteins of RNA silencing pathways, which regulate gene expression in a sequence-
350 specific manner (Duan et al. 2015). RNA silencing is also the main antiviral defense mechanism
351 possessed by plants. It can be post-transcriptional (PTGS) or transcriptional (TGS) (Carbonell
352 and Carrington 2015).

353 ***The qHBV11.1 region contains a gene for durable resistance to Rice stripe virus***

354 The genomic region of *qHBV11.1* contains many nucleotide binding site-leucine-rich repeat
355 (NBS-LRR) genes, which are broadly known to confer resistance to multiple diseases (McHale
356 et al. 2006). Other types of genes are also found in the interval, and remarkably the *STV11* gene
357 (MSU:LOC_Os11g30910, Chr11:17,984,964-17,986,719b; RAP-DB: Os11g0505300), which
358 confers durable resistance to *Rice stripe virus* (RSV), one of the most devastative viral diseases
359 of rice in Asia (Wang et al. 2014). Interestingly, this virus belongs to the same genus as RHBV
360 and it is also transmitted by planthoppers (*Laodelphax striatellus* Fallen). It should be also
361 noted that, very close to the *qHBV11.1* support interval, there are several paralog histidine
362 kinase/Hsp90-like ATPase genes (MSU:LOC_Os11g31480, MSU:LOC_Os11g31500) that also
363 confer resistance to RSV (Hayano-Saito and Hayashi, 2020).

364 DISCUSSION

365 Successful genotype-phenotype association studies require precise methodologies to assess
366 phenotypic variables. The latest technological advances in image acquisition have allowed the
367 development of computer tools for picture processing and analysis that provide accurate data.
368 Image processing for quantifying damage caused by plant diseases is particularly useful as it
369 advantageously replaces traditional scoring scales, which are too dependent on the observer.
370 The RHB disease has been commonly evaluated using the percentage of diseased plants at a
371 given time – that is, the incidence. However, the main drawback of this approach is that it
372 classifies all the plants with symptoms in the same class, without considering the level of
373 damage – the severity. Understanding the genetic mechanisms of resistance to the *hoja blanca*
374 disease therefore requires proper assessment of not only its incidence but also its severity. In
375 this sense, we proposed for the first time the use of digital images to evaluate the severity of
376 damage caused by RHB by estimating the affected leaf area. We showed that severity varies
377 continuously among F_3 families, a characteristic behavior of quantitative features. Severity and
378 incidence evaluation allowed us to identify different QTLs, allowing us to better explain the

379 complexity of the genetics of resistance to RHB. Keeping in mind that the parents of the four
380 populations were among the most resistant of a larger panel (Cruz et al. 2018), and although
381 significant differences between incidence and severity were found among the parents of the
382 four populations, complete resistance was not observed, confirming a previous observation by
383 (Morales and Jennings 2010) about the lack of complete resistance to RHB in the *O. sativa*
384 genepool.

385 **RHB resistance is regulated by multiple QTLs**

386 The QTLs found in this study show that resistance to RHB, assessed both by affected leaf area
387 and incidence, is controlled by multiple genes. The co-location of LOD score peaks for incidence
388 in the same region of chromosome 4 in three different crosses suggests that it is likely the same
389 QTL, namely *qHBV4.1*. Although *qHBV4.1* was associated to both phenotypic variables, its
390 association was greater with incidence where it explained up to 63.6% of the phenotypic
391 variance. These results suggest that the main action of *qHBV4.1* could take place in the first
392 phase of the interaction of the virus with the plant, preventing the virus to enter and propagate
393 in the plant, which is reflected in a smaller number of plants with symptoms. In addition, the
394 little variation in nucleotides – less than 1% – in the region of *qHBV4.1*, between Badka and PTB
395 25 indicates a probable common local ancestry (Figure S3). The differences in the LOD score
396 (5.83 *vs.* 8.26) and in R^2 values (21.4% *vs.* 36.6%) for ALA, in these two populations, could be
397 explained by the difference in the percentage of virulence of the vector colonies, which were
398 ~69% and ~46% for Badka × BBT 50 and PTB 25 × BBT 50, respectively. Also, the phenotypic
399 evaluation trials were performed at different times of the year for the different populations.
400 This involves the use of different vector colonies, and implies variations in microenvironmental
401 factors such as day and night temperature, radiation or humidity that might affect the behavior
402 of the insect and its ability to transmit the virus.

403 A major QTL had been previously identified in the region of *qHBV4.1* in the varieties FD 2000
404 and Fedearroz 50 by incidence assessment (Romero et al. 2014), which suggests a
405 predominant, common mechanism of resistance to RHBV in the different clades of *Oryza sativa*.
406 The genetic variation between the parents observed in this region shows that they carry
407 different alleles, of *japonica* and *indica* origins. This has implications for crop improvement,
408 allowing breeders to broaden the genetic base of resistance in elite germplasm. A QTL for
409 resistance to *Rice stripe virus* (RSV) has been identified between 4.4 and 6.9 Mpb in the N22 Aus
410 variety, explaining 13.4% of the trait variance (Wang et al. 2013). The *qHBV4.1* QTL region
411 might thus contain at least two tenuivirus resistance genes. As mentioned above, in the region
412 of *qHBV4.1* there is a putative candidate gene that encodes for the AGO-4 Argonaute protein
413 (LOC_Os04g06770). AGO proteins, in addition to be regulatory factors of endogenous gene
414 expression, also play a critical role in the defense against viruses through interference with
415 small RNA of viral origin which bind to AGOs and serve as a guide for it to cut new viral RNA
416 particles (Mallory and Vaucheret 2011)(Silva-Martins et al., 2020). This system is a common
417 defense mechanism against pathogens, and AGO-4 might well be associated with resistance to
418 RHBV. Moreover, Bhattacharjee et al. (2009) showed, in *Nicotiana benthamiana*, that Argonaute
419 proteins can interact with viral transcripts to alter virus resistance mediated by proteins

420 containing nucleotide-binding/leucine-rich repeats domains. We are currently carrying
421 CRISPR-Cas9 knock-out experiments in AGO-4 in order to test this hypothesis.

422 A distinct QTL for RHB incidence on chromosome 4, *qHBV4.2*^{WAS}, was identified in the WAS 208
423 × BBT 50 cross. This QTL was also a major one, explaining ~50% of the phenotypic variation.
424 The region contains genes associated with cold tolerance (SAPK7) (Basu and Roychoudhury,
425 2014) and photo-oxidative stress (OsAPX7)(Caverzan et al. 2014), and a more interesting gene
426 encoding for a zinc finger-type C3H protein (LOC_Os04g35800). This class of proteins has been
427 found to be associated with resistance viruses in animals through degradation of viral RNA (Gao
428 et al. 2002; Mao et al. 2013). Although there are no reports so far of its involvement in resistance
429 to viruses in plants, it has been found to be associated with response to other types of pathogens
430 (and abiotic stress) (Deng et al. 2012; Jan et al. 2013), which makes it an interesting candidate
431 for RHB resistance. Another candidate is a gene encoding for a MAPKKK kinase, which belongs
432 to a signaling cascade that plays a major role in disease resistance in eukaryotes. This gene is
433 also an interesting candidate because the activation of MAPK proteins occurs in the earliest
434 stages after the interaction of the pathogen with the plant (Meng and Zhang 2013), which
435 coincides well with the identification of this QTL through the assessment of incidence, but not
436 severity, indicating that it – like *qHBV4.1* – could exert its action in the early stages of the
437 interaction of RHBV with the plant.

438 In contrast with the two QTLs identified on chromosome 4 that are predominantly associated
439 with incidence, *qHBV11.1* has a greater effect on disease severity. This could suggest a later
440 action, in a second stage of the interaction of the plant with the virus or the insect vector, after
441 the virus manages to enter the cells and to propagate. In this scenario *qHBV11.1* would have a
442 key role in diminishing the damage caused by the virus. This is thus more a "tolerance QTL".

443 It has been proposed that the resistance to RHB comes mostly from *japonica* germplasm
444 (Morales and Jennings 2010). If this was the case, and to explain that the resistance sources
445 studied here are of *indica* type, one would need to assume that the region of *qHBV11.1* was
446 inherited from *japonica* through introgression into *indica*. This is not supported by the
447 clustering analysis, which showed that the WAS 208 and Badka parents, for this region, are
448 grouped together with *indica* type accessions such as IR8. Therefore, this QTL does not
449 originate from the *japonica* cluster.

450 A search for candidate genes for *qHBV11.1* evidenced a co-localization with a QTL for resistance
451 to *Rice stripe virus* (RSV) found in different genetic backgrounds: in the *indica* varieties Teqing
452 (*qSTV11*^{TQ}) (Wu et al. 2011) and Shingwang (*qSTV11*^{SG}) (Kwon et al. 2012), the Aus varieties
453 Kasalath (*qSTV11*^{KAS}) (Zhang et al. 2011), N22 (*qSTV11.1*) (Wang et al. 2013) and Dular (Wu et
454 al. 2011), the *japonica* Kanto 72 (Maeda et al. 2006), and *O. rufipogon* (Wang et al. 2014).
455 Whether those QTLs correspond to the same locus or to different, linked genes still needs to be
456 clarified. The hypothesis of a common defense mechanism acting against RHBV and RSV seems
457 plausible, as both are RNA viruses of the same genus, although it has been found that RHBV is
458 more related to other tenuiviruses like *Echinochloa hoja blanca virus* (EHBV) and *Urochloa hoja*
459 *blanca virus* (UHBV) than to RSV (Fauquet et al., 2005), besides not being serologically related
460 (Morales and Jennings 2010). Further studies of fine mapping and cloning of *qSTV11*^{KAS} showed

461 that the gene responsible for resistance to RSV encodes a sulfotransferase that catalyzes the
462 conversion of salicylic acid to its sulfated form. Although it is not clear how this process confers
463 resistance against the virus, it was found that the susceptible allele of this gene is not capable
464 of inducing this conversion (Wang et al. 2014). Salicylic acid has been found to be essential in
465 the initiating signal to activate systemic resistance against *Tobacco mosaic virus* (Zhu et al.
466 2014), and also plays a central role in the hypersensitive response against *Potato virus Y* (PVY)
467 (Baebler et al. 2014). It has even been reported as a direct inhibitor of the replication of *Tomato*
468 *bush dwarf virus* (TBSV) (Tian et al. 2015). It is thus plausible that the *STV11* gene is involved
469 in resistance to RHBV. In all cases, Wang et al demonstrated that the *STV11* gene inhibits the
470 replication of the RSV, which could explain the fact that the QTL LOD score is higher for ALA
471 than for incidence in Badka and WAS208. We are currently analyzing knock-out lines obtained
472 by CRISPR-Cas9 in STV11 to verify this hypothesis.

473 A second QTL on chromosome 11, *qHBV11.2*, was identified for disease incidence in the two
474 crosses involving WAS 208 and PTB 25. Based on the variation found in the clustering analysis
475 – and assuming the QTL is the same in the two crosses – it is possible that WAS 208 and PTB 25
476 have different allelic variants of *qHBV11.2* with a different effect on disease resistance, which
477 could explain that in PTB 25 it was also associated with severity. The region could also
478 correspond to two distinct, linked QTLs in the two populations, since their support intervals
479 are quite large (> 3 Mpb). To answer this question, a fine mapping study of the region using
480 larger F_2 populations would be needed.

481 An additional QTL for RHB incidence, *qHBV6*, was identified In the PTB 25 × BBT 50 cross on
482 chromosome 6. In a previous GWAS experiment, the same region was identified in the
483 genotypes PTB 25 and Pokkali (Cruz-Gallego et al. 2018), also supported by a biparental QTL
484 analysis in the $F_{2:3}$ cross FD 50 × WC 366 (our unpublished data). A search for genes in this
485 region found the OsBBI1 gene that participates in various biological processes, among which is
486 the innate immune response. OsBBI1's expression is induced by the fungus *Magnaporthe oryzae*
487 and chemical inducers such as salicylic acid (Li et al. 2011), which, as discussed above, is also
488 associated with systemic resistance to viruses. OsBBI1 is thus a good candidate gene for *qHBV6*.

489 **Resistance QTLs in the susceptible parent**

490 In the PTB 25 × BBT 50 population, two QTLs for RHB incidence were identified on
491 chromosomes 9 and 10, of which the allele that reduces the affected leaf area is brought by
492 BBT 50. One explanation could be that PTB 25 carries susceptibility alleles at these QTLs.
493 However, this is unlikely since inactivation of a susceptibility gene by the resistant allele results
494 in increased resistance. Genetically, the resistant allele of a susceptibility gene is therefore
495 generally recessive. This is not what we observed, since the mean ALA of the heterozygous class
496 AB is more similar to the susceptible class AA (PTB 25) than to the BB class (BBT 50). Therefore,
497 the most likely explanation is that the three other resistant parents (FD 2000, WC 366 and
498 Badka) and the susceptible parent (BBT 50) carry resistant alleles at these QTL, while the
499 PTB 25 parent does not.

500 **Integration of QTLs into a RHB disease resistance model**

501 Based on the QTLs associated with RHB resistance, we propose a simplistic model that draws
502 the possible processes involving these loci. The QTLs *qHBV4.1* and *qHBV4.2* were found to be
503 most associated with disease incidence, so it is likely that they are involved in the first phase of
504 virus-plant interaction. These QTL may be inhibiting the translation of viral RNA, either by
505 direct action on them or through other genes for degradation. The effect of these QTLs on the
506 incidence, indicates that this mechanism might be the most important for the resistance of the
507 plant to the virus. In the scenario where the favorable alleles of *qHBV4.1* or *qHBV4.2* are not
508 present or that the virus manages to overcome this barrier and to propagate in the plant, an
509 additional mechanism involving *qHBV11.1* would be hampering the multiplication of the virus.
510 This could occur by direct action, inhibiting the synthesis of new viral particles, or more likely,
511 serving as a trigger signal for the activation of defense genes of the systemic resistance system.
512 Although this mechanism would not provide complete resistance to the virus, it would
513 considerably reduce the damage – meaning less leaf area affected. The *qHBV6* QTL is also
514 related to the severity of the disease, so it is possible that it also participates in this same
515 mechanism.

516 CONCLUSION

517 Altogether these results show that resistance to RHB disease is controlled by multiple
518 quantitative genetic factors of different origins, with varying effects and action mode. The
519 identification of strong candidate genes underlying the detected QTLs supports the idea that
520 resistance is mediated by different defense mechanisms such as viral gene silencing and the
521 salicylic acid pathway. This hypothesis has proven true for other study models such as in the
522 *Citrus tristeza virus* (CTV) where it has been found that silencing of key genes in these defense
523 pathways increases the spread of the virus and its accumulation in the plant (Gómez-Muñoz et
524 al. 2017). Regarding the identification of the genetic mechanisms of resistance, our study lacks
525 long-reads based sequencing data in the resistant and susceptible parental lines. Generating
526 such data would allow structural analysis to identify copy number variations for the candidate
527 genes, as well as comparison of resistant and susceptible alleles at the nucleotide and aminoacid
528 levels.

529 A considerable amount of work is still needed to understand the fine mechanisms behind
530 defense against RHB. In particular, it will be necessary to clarify whether some of the QTLs
531 found in this study are actually acting against the insect vector, and not the virus itself. Indeed,
532 insect resistance by antixenosis and/or antibiosis are known to be present in rice (see Figure 1
533 in Fujita et al. 2013) and overlap with some of our QTLs.

534 Finally, the QTLs detected in this study will benefit the rice breeder's community. Marker-
535 assisted selection can be used to combine several resistance QTLs to HBV with other traits,
536 using for instance a pyramiding approach, or other types of marker-assisted selection.

537 ## LIST OF ABBREVIATIONS

538 ALA: affected leaf area
539 Badka: Badkalamkati variety, accession number IRGC 45011
540 BBT 50: Bluebonnet 50 variety
541 CIAT: Centro Internacional de Agricultura Tropical (now Alliance Bioversity-CIAT)
542 CIM: composite interval mapping
543 cM: centimorgan
544 CTV: *Citrus tristeza virus*
545 DAI: days after infestation
546 DNA: deoxyribonucleic acid
547 EDTA: ethylenediaminetetraacetic acid
548 EHBV: *Echinochloa hoja blanca virus*
549 FD 50: Fedearroz 50 variety, accession number IRGC 1799-1-1
550 FD 2000: Fedearroz 2000 variety, accession number IRGC 124388
551 FLAR: Fondo Latinoamericano para Arroz de Riego
552 fsGBS: flexible and scalable genotyping by sequencing
553 IFC: integrated fluidic circuit
554 LOD: logarithm in base 10 of likelihoods odds
555 MATAB: mixed alkyltri-methylammonium bromide
556 MEG: maternally expressed gene
557 MLGM: generalized linear mixed model
558 NBS-LRR: nucleotide binding site-leucine-rich repeat
559 PCR: polymerase chain reaction
560 PTGS: post-transcriptional gene silencing
561 PTB 25: PTB 25 variety, accession number IRGC 6386
562 PVY: *Potato virus Y*
563 QTL: quantitative trait locus
564 RHB: rice *hoja blanca* disease
565 RHBV: *Rice hoja blanca virus*
566 RNA: ribonucleic acid
567 RSV: *Rice stripe virus*
568 SD: segregation distortion
569 SIM: simple interval mapping
570 SMR: single-marker regression
571 SNP: single nucleotide polymorphism
572 TBSV: *Tomato bush dwarf virus*
573 TGS: transcriptional gene silencing
574 UHBV: *Urochloa hoja blanca virus*
575 WAS 208: WAS 208-B-B-5-1-1-3 variety, accession number IRGC 121855
576 WGS: whole-genome sequencing

DECLARATIONS

Ethical Approval and Consent to participate

Not applicable

Consent for publication

Not applicable

Availability of supporting data

The datasets used and/or analyzed during the current study are available from the corresponding author on reasonable request.

Competing interests

The authors declare that they have no competing interests

Funding

The following programs partially supported this initiative: The Latin American Fund for Irrigated Rice (FLAR), the RICE CGIAR Research Program (RICE CRP), and the OMICAS program (Optimización Multiescala In-Silico de Cultivos Agrícolas Sostenibles (Infraestructura y Validación en Arroz y Caña de Azúcar), sponsored within the Colombian Scientific Ecosystem by the World Bank, The Colombian Ministry of Science, Technology and Innovation (MINCIENCIAS), ICETEX, The Colombian Ministry of Education and the Colombian Ministry of Industry and Tourism under GRANT ID: FP-44842-217-2018.

Authors' contributions

AS wrote the draft manuscript and performed the SNP design and QTL analysis, MEM set up the disease severity experiments, CQ supervised the SNP genotyping, JQ did the statistical treatment of phenotype data, JT led the Agrobiotechnology laboratory, EG led the FLAR, MC supervised the phenotyping experiments, ML designed the QTL experiments and edited the manuscript, MC and ML supervised AS work.

Acknowledgements

We warmly thank Drs. Laurence Albar, Sébastien Cunnac, Mathilde Hutin and Marlène Lachaux from the IRD for their useful comments on the manuscript. We also thank the two reviewers for their careful review that helped significantly improving the quality of the manuscript, and the associate editor for handling the submission.

REFERENCES

Baebler Š, Witek K, Petek M, et al (2014) Salicylic acid is an indispensable component of the Ny-1 resistance-gene-mediated response against *Potato virus Y* infection in potato. Journal of Experimental Botany 65:1095–1109. doi: 10.1093/jxb/ert447

610 Bhattacharjee, S, Zamora A, Tehseen Azhar MA, Sacco MA, Lambert LHMoffet, P (2009) Virus
611 resistance induced by NBS–LRR proteins involves Argonaute4-dependent translational
612 control. The Plant Journal 58:940-951. doi: 10.1111/j.1365-313X.2009.03832.x

613 Campbell CL, Neher DA (1994) Estimating disease severity and incidence. In: Epidemiology and
614 Management of Root Diseases (pp. 117-147). Springer, Berlin, Heidelberg.

615 Carbonell A, Carrington JC (2015) Antiviral roles of plant ARGONAUTES. Current Opinion in
616 Plant Biology 27:111–117. doi: 10.1016/j.pbi.2015.06.013

617 Caverzan A, Bonifacio A, Carvalho Fel, et al (2014) The knockdown of chloroplastic ascorbate
618 peroxidases reveals its regulatory role in the photosynthesis and protection under photo-
619 oxidative stress in rice. Plant Science 214:74–87. doi: 10.1016/j.plantsci.2013.10.001

620 Cruz-Gallego M, Rebolledo MC, Cuasquer JB, et al (2018) Identification of new sources of
621 resistance to RHBV - *Rce hoja blanca virus*. Acta Agronomica 67:368–374. doi:
622 10.15446/acag.v67n2.61334

623 Deng H, Liu H, Li X, et al (2012) A CCCH-type zinc finger nucleic acid-binding protein
624 quantitatively confers resistance against rice bacterial blight disease. Plant Physiology
625 158:876–889. doi: 10.1104/pp.111.191379

626 Duan C-G, Zhang H, Tang K, et al (2015) Specific but interdependent functions for Arabidopsis
627 *AGO4* and *AGO6* in RNA-directed DNA methylation. EMBO Journal 34:581–592. doi:
628 10.15252/embj.201489453

629 Duitama J, Quintero JC, Cruz DF, et al (2014) An integrated framework for discovery and
630 genotyping of genomic variants from high-throughput sequencing experiments. Nucleic
631 Acids Research 42:e44. doi: 10.1093/nar/gkt1381

632 Duitama J, Silva A, Sanabria Y, et al (2015) Whole genome sequencing of elite rice cultivars as a
633 comprehensive information resource for marker assisted selection. PLoS ONE
634 10:e0124617–20. doi: 10.1371/journal.pone.0124617

635 Falconer DS (1981) *Introduction to Quantitative Genetics*. Longman, New York.

636 Fisher RA (1932) *Statistical Methods for Research Workers*, 4th Edition. Oliver and Boyd,
637 Edinburgh

638 Fragoso CA, Moreno M, Wang Z, et al (2017) Genetic architecture of a rice Nested Association
639 Mapping population. G3 | Genes, Genomes, Genetics g3.117.041608–15. doi:
640 10.1534/g3.117.041608

641 Fujita G, A Kohli, F. G. Horgan (2013) Rice Resistance to Planthoppers and Leafhoppers. Critical
642 Reviews in Plant Sciences, 32:162–191. doi: 10.1080/07352689.2012.735986

643 Gao G, Guo X, Goff SP (2002) Inhibition of retroviral RNA production by ZAP, a CCCH-type zinc
644 finger protein. Science 297:1703–1706. doi: 10.1126/science.1074276

645 Gómez-Muñoz N, Velázquez K, Vives MC, et al (2017) The resistance of sour orange to *Citrus*
646 *tristeza virus* is mediated by both the salicylic acid and RNA silencing defence pathways.
647 Molecular Plant Pathology 18:1253–1266. doi: 10.1111/mpp.12488

648 Hayano-Saito, Y., Hayashi, K., 2020. Stvb-i, a Rice Gene Conferring Durable Resistance to Rice
649 stripe virus, Protects Plant Growth From Heat Stress. Front. Plant Sci. 11, 519.
650 https://doi.org/10.3389/fpls.2020.00519

651 Silva-Martins, G., Bolaji, A., Moffett, P., 2020. What does it take to be antiviral? An Argonaute-
652 centered perspective on plant antiviral defense. J. Exp. Bot. 71, 6197–6210.
653 https://doi.org/10.1093/jxb/eraa377

654 Heffelfinger C, Fragoso CA, Lorieux M (2017) Constructing linkage maps in the genomics era
655 with MapDisto 2.0. Bioinformatics 1–2. doi: 10.1093/bioinformatics/btx177

656 Heffelfinger C, Fragoso CA, Moreno MA, et al (2014) Flexible and scalable genotyping-by-
657 sequencing strategies for population studies. BMC Genomics 15:979. doi: 10.1186/1471-
658 2164-15-979

659 Jan A, Maruyama K, Todaka D, et al (2013) OsTZF1, a CCCH-tandem zinc finger protein, confers
660 delayed senescence and stress tolerance in rice by regulating stress-related genes. Plant
661 Physiology 161:1202–1216. doi: 10.1104/pp.112.205385

662 Joehanes R, Nelson JC (2008) QGene 4.0, an extensible Java QTL-analysis platform.
663 Bioinformatics 24:2788–2789. doi: 10.1093/bioinformatics/btn523

664 Kosambi DD (1944) The Estimation of Map Distances from Recombination Values. Annals of
665 Eugenics 12:172–175.

666 Kwon T, Lee J-H, Park S-K, et al (2012) Fine mapping and identification of candidate rice genes
667 associated with *qSTV11*$^{(SG)}$, a major QTL for rice stripe disease resistance. Theoretical and
668 Applied Genetics 125:1033–1046. doi: 10.1007/s00122-012-1893-8

669 Li J-Y, Wang J, Zeigler RS (2014) The 3,000 rice genomes project: new opportunities and
670 challenges for future rice research. Gigascience 3:1–3. doi: 10.1186/2047-217X-3-8

671 Li W, Zhong S, Li G, et al (2011) Rice RING protein OsBBI1 with E3 ligase activity confers broad-
672 spectrum resistance against *Magnaporthe oryzae* by modifying the cell wall defence. Cell
673 Research 21:835–848. doi: 10.1038/cr.2011.4

674 Lorieux M (2012) MapDisto: fast and efficient computation of genetic linkage maps. Molecular
675 Breeding 30:1231–1235. doi: 10.1007/s11032-012-9706-y

676 Lorieux M (2018) Is this a fake QTL? A short note on analysis of multiple QTL peaks on the same
677 chromosome. BioRXiv 1–7. doi: 10.1101/270736

678 Lorieux M (2021) Direct fast estimator for recombination frequency in the F_2 cross. BioRXiv 1–
679 10. doi: 10.1101/2021.04.20.440219

680 Maeda H, Matsushita K, Iida S, Sunohara Y (2006) Characterization of two QTLs controlling
681 resistance to *Rice stripe virus* detected in a Japanese upland rice line, Kanto 72. Breeding
682 Science 56:359–364. doi: 10.1270/jsbbs.56.359

683 Mallory A, Vaucheret H (2011) Form, function, and regulation of ARGONAUTE proteins. The
684 Plant Cell Online 22:3879–3889. doi: 10.1105/tpc.110.080671

685 Mao R, Nie H, Cai D, et al (2013) Inhibition of hepatitis B virus replication by the host zinc finger
686 antiviral protein. PLoS Pathogens 9:e1003494. doi: 10.1371/journal.ppat.1003494

687 McHale L, Tan X, Koehl P, Michelmore RW (2006) Plant NBS-LRR proteins: adaptable guards.
688 Genome Biology 7:212–11. doi: 10.1186/gb-2006-7-4-212

689 Meng X, Zhang S (2013) MAPK cascades in plant disease resistance signaling. Annual Review of
690 Phytopathology 51:245–266. doi: 10.1146/annurev-phyto-082712-102314

691 Morales F and Jennings P (2010) Rice hoja blanca: a complex plant-virus-vector pathosystem.
692 CAB Reviews. doi: 10.1079/PAVSNNR20105043

693 Prins P, Jansen RC, Broman KW (2010) R/qtl: high-throughput multiple QTL mapping.
694 Bioinformatics 26:2990–2992. doi: 10.1093/bioinformatics/btq565

695 Risterucci AM, Grivet L, N'Goran J, et al (2000) A high-density linkage map of *Theobroma cacao*
696 L. Theoretical and Applied Genetics 101:948-955

697 Romero LE, Lozano I, Garavito A, et al (2014) Major QTLs control resistance to *Rice hoja blanca*
698 *virus* and its vector *Tagosodes orizicolus*. G3 | Genes, Genomes, Genetics 4:133–142. doi:
699 10.1534/g3.113.009373

700 Santos JD, Chebotarov D, McNally KL, Bartholomé J, Droc G, Billot C, Glaszmann JC (2019) Fine
701 Scale Genomic Signals of Admixture and Alien Introgression among Asian Rice Landraces.
702 Genome Biology and Evolution 11: 1358–1373. doi: 10.1093/gbe/evz084

703 Tian M, Sasvari Z, Gonzalez PA, et al (2015) Salicylic acid inhibits the replication of *Tomato*
704 *bushy stunt virus* by directly targeting a host component in the replication complex.
705 Molecular Plant-Microbe Interactions 28:379–386. doi: 10.1094/MPMI-09-14-0259-R

706 Wang Q, Liu Y, He J, et al (2014) *STV11* encodes a sulphotransferase and confers durable
707 resistance to *Rice stripe virus*. Nature Communications 5:4768. doi: 10.1038/ncomms5768

708 Wang Q, Liu Y, Hu J, et al (2013) Detection of quantitative trait loci (QTLs) for resistances to
709 small brown planthopper and *Rice Stripe Virus* in rice using recombinant inbred lines.
710 International journal of molecular sciences 14:8406–8421. doi: 10.3390/ijms14048406

711 Wang S, Tan Y, Tan X, et al (2009) Segregation distortion detected in six rice F_2 populations
712 generated from reciprocal hybrids at three altitudes. Genetics Research 91:345–353. doi:
713 10.1017/S0016672309990176

714 Wu X, Zuo S, Chen Z, et al (2011) Fine mapping of $qSTV11^{TQ}$, a major gene conferring resistance
715 to rice stripe disease. Theoretical and Applied Genetics 122:915–923. doi:
716 10.1007/s00122-010-1498-z

717 Yamamoto E, Yonemaru J-I, Yamamoto T, Yano M (2012) OGRO: The overview of functionally
718 characterized genes in rice online database. Rice 5:1–10. doi: 10.1186/1939-8433-5-26

719 Zhang Y-X, Wang Q, Jiang L, et al (2011) Fine mapping of qSTV11 KAS , a major QTL for rice
720 stripe disease resistance. Theoretical and Applied Genetics 1–14. doi: 10.1007/s00122-
721 011-1557-0

722 Zhu F, Xi D-H, Yuan S, et al (2014) Salicylic acid and jasmonic acid are essential for systemic
723 resistance against *Tobacco mosaic virus* in *Nicotiana benthamiana*. Molecular Plant-
724 Microbe Interactions 27:567–577. doi: 10.1094/MPMI-11-13-0349-R

725

726

727

TABLES

Table 1 Summary of genetic maps characteristics in the four F_2 populations. Map sizes are expressed in centimorgans (cM) calculated with the Kosambi mapping function

Cross	*Population size*	*Number SNPs*	*Number SSRs*	*Total markers*	*Map size (cM)*
WAS 208 × BBT 50	104	207	2	209	1,296
Badka × BBT 50	105	226	1	227	1,570
PTB 25 × BBT 50	108	184	1	185	1,617
FD 2000 × BBT 50	105	217	0	217	1,630

Table 2 Trait correlation values in each population, and in the four F_2 populations combined. The '_M0' and '_V1' suffixes stand for normalized and centralized data, respectively

A. WAS 208 × BBT50

	SEVERITY
INCIDENCE	0.42

B. Badka × BBT50

	SEVERITY
INCIDENCE	0.625

C. PTB 25 × BBT50

	SEVERITY
INCIDENCE	0.458

D. FD 2000 × BBT50

	SEVERITY
INCIDENCE	0.655

E. Four crosses combined

	INCIDENCE	*INCIDENCE_ M0_V1*	*SEVERITY*	*SEVERITY _M0_V1*
INCIDENCE	1	0.891	0.613	0.481
INCIDENCE_M0_V1	0.891	1	0.449	0.538
SEVERITY (ALA)	0.613	0.449	1	0.829
SEVERITY_M0_V1	0.481	0.538	0.829	1

Table 3 Summary statistics for QTLs detected with Simple Interval Mapping (SIM) analysis in the four F_2 crosses, and joint analysis, with Qgene version 4.40. Positions in Mbp on Nipponbare genome (MSU v7). Empirical threshold $\alpha_{0.01}$ calculated with 10,000 permutations. R^2: part of the trait variance explained by the QTL. A: Additivity effect. D: Dominance effect. QTLs that were detected with Composite Interval Mapping (CIM) but not with SIM appear in pale gray

Trait	*QTL name*	*WAS 208*	*Bad-ka*	*PTB 25*	*FD 2000*	*Joint (4 pop.)*	*Chromo-some*	*Peak (Mbp)*	R^2	*Additivity (A)*	*Dominance (D)*	*|D /A |*	*LOD score*	*Permutation threshold α = 0.01*
Incidence	*qHBV4.1*		✓				4	3.56-6.47	0.63	-24.14	-1.17	0.05	20.97	4.43
				✓				0.22-4.19	0.60	-24.47	-5.24	0.21	21.26	4.55
					✓			3.56-3.57	0.34	-14.69	-0.46	0.03	9.11	4.40
						✓		3.56-3.57	0.42	-17.51	-2.51	0.14	47.00	4.50
Incidence	*qHBV4.2* ^{WAS208}	✓					4	21.8	0.52	-18.44	4.90	0.27	15.49	4.47
Incidence	*qHBV6.1* ^{PTB25}			✓			6	1.87-3.08	0.15	-16.79	-3.69	0.22	3.64	4.55
Incidence	*qHBV11.1*				✓		11	18.78-18.87	0.29	-14.25	-3.50	0.25	7.43	4.40
						✓		18.5	0.11	-9.33	-4.11	0.44	10.40	4.37
Incidence	*qHBV11.2*	✓					11	7.43-17.23	0.09	-8.51	1.98	0.23	2.08	4.47
				✓				7.43-8.60	0.09	-9.58	-6.68	0.70	2.16	4.55
ALA	*qHBV4.1*		✓				4	3.56-6.47	0.31	-13.90	0.43	0.03	8.31	4.49
				✓				0.22-4.19	0.30	-10.86	-5.41	0.50	8.50	4.29
					✓			3.71-4.19	0.25	-9.16	-3.73	0.41	6.69	4.40
						✓		3.71-4.19	0.23	-9.46	-3.95	0.42	23.40	4.30
ALA	*qHBV11.1*	✓					11	18.06	0.21	-8.82	-3.17	0.36	5.32	4.56
			✓					17.62-17.83	0.19	-10.70	-2.33	0.22	4.68	4.49
					✓			18.06	0.33	-9.36	-7.18	0.77	8.98	4.69
						✓		18.06	0.17	-8.65	-3.62	0.42	17.29	4.37

743 **Table 4** Summary statistics for QTLs detected with Composite Interval Mapping (CIM) analysis in the four F_2 crosses, and joint analysis, with Qgene
744 version 4.40. Cofactor selection method: Forward selection, automatic, QTL cofactors instead of markers = no. Positions in Mbp on Nipponbare
745 genome (MSU v7). Empirical threshold $\alpha_{0.01}$ calculated with 10,000 permutations. R^2: part of the trait variance explained by the QTL. A: Additivity
746 effect. D: Dominance effect.

Trait	*QTL name*	*WAS 208*	*Bad-ka*	*PTB 25*	*FD 2000*	*Joint (4 pop.)*	*Chromo-some*	*Peak (Mbp)*	R^2	*Additivity (A)*	*Dominance (D)*	*|D /A |*	*LOD score*	*Permutation threshold α = 0.01*
Incidence	*qHBV4.1*		✓				4	3.56-4.46	0.6	-22.37	-0.67	0.03	23.46	5.57
				✓				3.5-4.19	0.73	-25.38	-6.84	0.27	30.45	5.10
					✓			3.5-3.7	0.501	-14.95	1.34	0.09	17.27	4.95
						✓		3.5-3.7	0.42	-16.78	-1.09	0.06	47.82	4.85
Incidence	*qHBV4.2* ^{WAS208}	✓					4	21.29-21.81	0.57	-18.75	3.15	0.17	18.31	5.47
Incidence	*qHBV6.1* ^{PTB25}			✓			6	0.18-1.76	0.25	-10.52	0.16	0.02	9.71	5.11
Incidence	*qHBV11.1*				✓		11	17.8-18.52	0.44	-13.83	-5.4	0.39	14.08	5.29
						✓		17.8-18.52	0.08	-7.154	-3.314	0.46	7.26	4.32
Incidence	*qHBV11.2*	✓					11	7.43-17.23	0.21	-8.16	2.66	0.33	5.02	4.11
				✓				7.43-16.6	0.242	-10.21	2.45	0.24	5.90	4.97
ALA	*qHBV4.1*		✓				4	3.56-4.46	0.26	-10.65	-2.86	0.27	8.98	5.26
				✓				3.56-4.19	0.26	-9.53	-1.07	0.11	9.81	5.43
					✓			3.56-4.46	0.29	-7.87	-2.48	0.32	9.93	5.32
						✓		3.56-4.46	0.222	-8.958	-2.899	0.32	23.00	5.33
ALA	*qHBV11.1*	✓					11	18.0-18.8	0.19	-8.71	-2.94	0.34	5.32	4.84
			✓					17.8-18.5	0.23	-10.27	-3.19	0.31	6.09	4.95
					✓			17.8-18.5	0.37	-8.74	-7.01	0.80	11.52	5.47
						✓		18.06	0.19	-8.03	-2.92	0.36	18.84	4.62

747

Table 5 Summary statistics for QTLs detected with Simple Marker Regression (SMR) analysis in the four F_2 crosses, joint- and meta-analyses, with MapDisto version 2.0. Positions in Mbp on Nipponbare genome (MSU v7). Empirical threshold $\alpha_{0.01}$ calculated with Qgene 4.40, with 10,000 permutations*. R^2: part of the trait variance explained by the QTL. A: Additivity effect. D: Dominance effect. QTLs that were detected with Composite Interval Mapping (CIM) but not with SMR appear in pale gray

Trait	*QTL name*	*WAS 208*	*Bad-ka*	*PTB 25*	*FD 2000*	*Joint (4 pop.)*	*Meta (4 pop.)*	*Chromo-some*	*Peak (Mbp)*	R^2	*Additivity (A)*	*Dominance (D)*	*|D /A |*	*F-test*	*-Log $_{10}$ (p-value of test)*	*Permutation threshold α = 0.01*
Incidence	*qHBV4.1*		✓					4	3.56-6.47	0.61	22.43	-1.65	0.07	74.18	19.33	4.35
				✓					0.22-4.19	0.60	24.47	-5.24	0.21	77.85	20.67	4.18
					✓				3.56-3.57	0.34	14.69	-0.46	0.03	25.29	8.84	4.20
						✓			3.56-3.57	0.42	17.51	-2.51	0.14	142.30	46.65	4.29
							✓		3.56-3.57	-	-	-	-	-	47.00	*
Incidence	*qHBV4.2* ^{WAS208}	✓						4	21.8	0.50	17.67	4.40	0.25	48.04	14.42	4.28
Incidence	*qHBV6.1* ^{PTB25}			✓				6	2.97-3.08	0.13	15.04	-6.76	0.45	7.82	3.16	4.31
Incidence	*qHBV11.1*				✓			11	18.78-18.87	0.29	14.09	-2.92	0.21	19.45	7.10	4.22
						✓			18.52-18.87	0.11	9.33	-4.11	0.44	25.24	10.32	4.29
							✓		18.52-18.87	-	-	-	-	-	8.91	*
Incidence	*qHBV11.2*	✓						11	7.43-17.23	0.10	7.55	2.05	0.27	5.12	2.11	4.29
				✓					7.43-8.60	0.09	9.15	-6.09	0.67	5.03	2.08	4.25
ALA	*qHBV4.1*		✓					4	3.56-6.47	0.29	12.85	-1.09	0.09	21.12	7.67	4.23
				✓					0.22-4.19	0.30	10.54	-2.48	0.24	22.09	8.01	4.18
					✓				3.71-4.19	0.25	8.86	-3.19	0.36	17.23	6.45	4.38
						✓			3.56-3.71	0.23	9.46	-3.95	0.42	60.94	23.23	4.22
							✓		3.70-4.19	-	-	-	-	-	20.75	*
ALA	*qHBV11.1*	✓						11	18.06	0.21	8.82	-3.17	0.36	13.43	5.17	4.31
			✓						17.62-17.83	0.19	10.70	-2.33	0.22	11.62	4.55	4.16
					✓				18.06	0.32	9.22	-6.66	0.72	23.72	8.46	4.38
						✓			18.06	0.17	8.65	-3.62	0.42	43.49	17.16	4.30
							✓		18.06	-	-	-	-	-	15.40	*

*Meta-analysis not available in Qgene

FIGURES

Figure 1 RHB disease severity (% of affected leaf area, ALA) measurement workflow. A: Image acquisition of rice leaves affected by RHB. B: Image segmentation to separate healthy from affected leaf areas. C: Healthy leaf area binarization. D: Total leaf area binarization

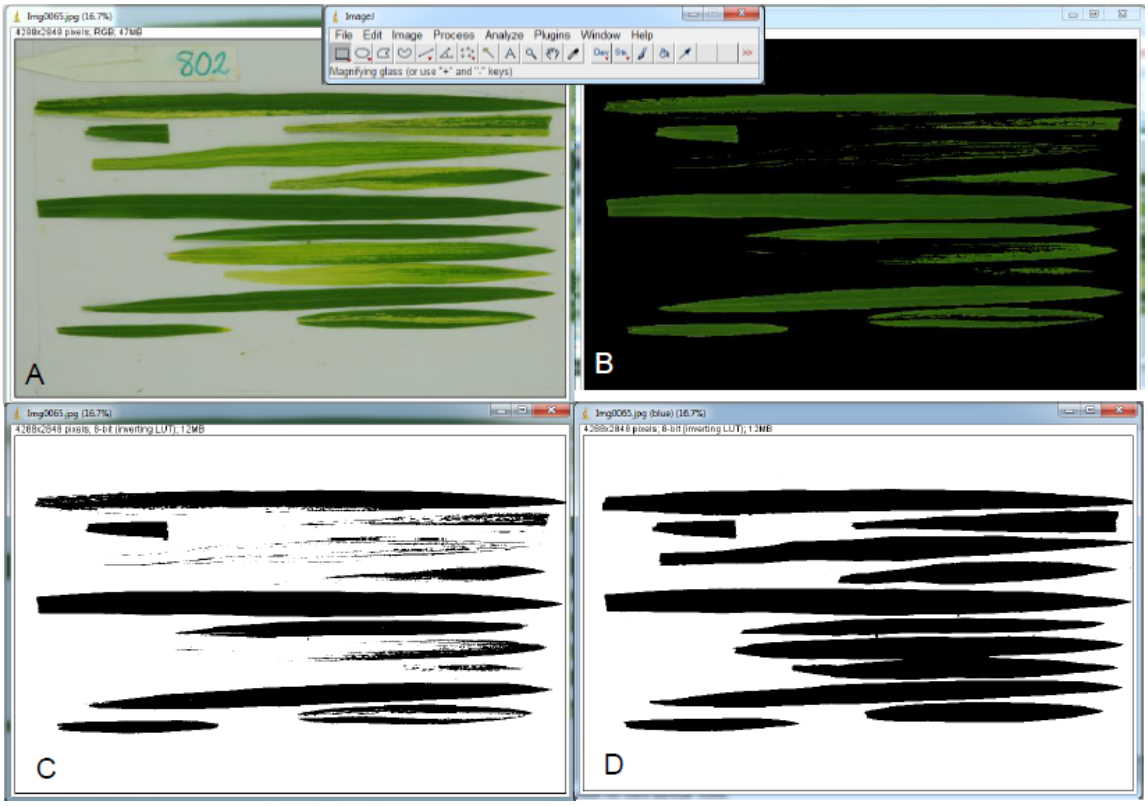

Figure 2 Distribution of the means of RHB incidence (% of plants with symptoms) and severity (% of affected leaf area, ALA) in F_3 families, in four *indica* × *japonica* rice mapping populations. Associated quantile-quantile plot to the right of every distribution. Means in F_3 families were calculated from 60 plants (incidence) or 10 plants (ALA). The green and orange arrows represent the average of the resistant and susceptible parents, respectively.

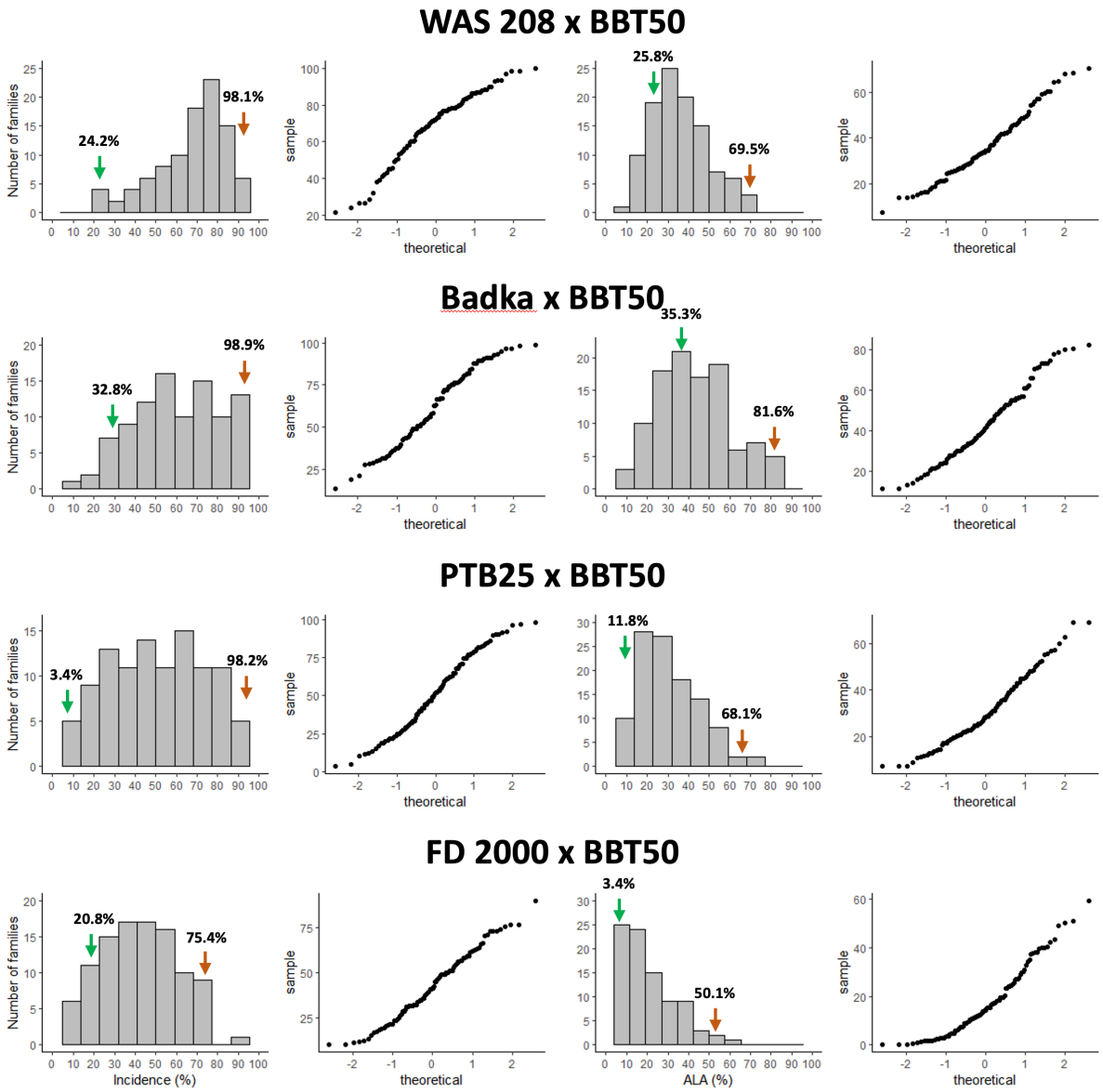

Figure 3 Whole-genome QTL plots (SIM) in the four crosses analyzed independently (A-D), and jointly (E). Red:incidence; purple: severity (ALA)

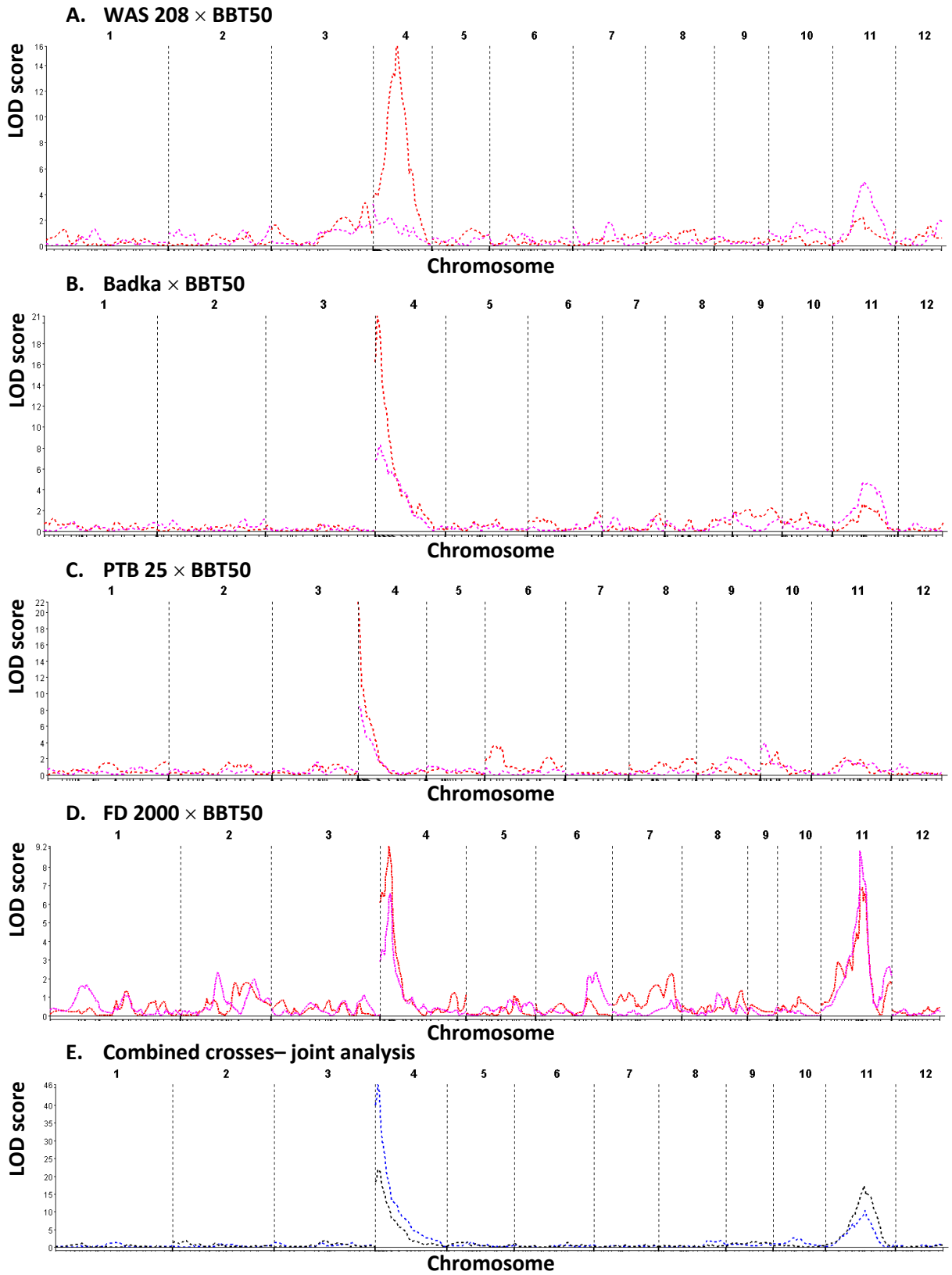

Figure 4 Hypothetical model of plant resistance mechanisms to RHBV

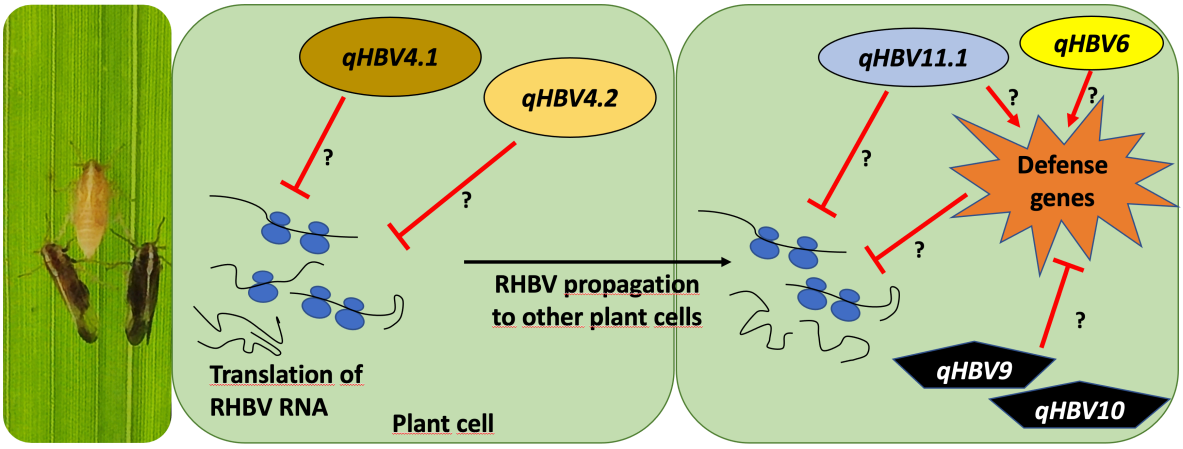

SUPPLEMENTAL FIGURES

Figure S1 Segregation distortion in several chromosomes, in the F_2 four populations. The X axis represents the position in cM on the chromosome. The Y axis is the frequency of the three F_2 genotypes: f(A): homozygous female parent (resistant to HBV); f(B): homozygous male parent BB 50 (susceptible to HBV); f(H): heterozygous. One clearly sees the departure from the expected genotypic frequencies, which in the F_2 cross are 0.25, 0.25 and 0.5 for f(A), f(B) and f(H), respectively.

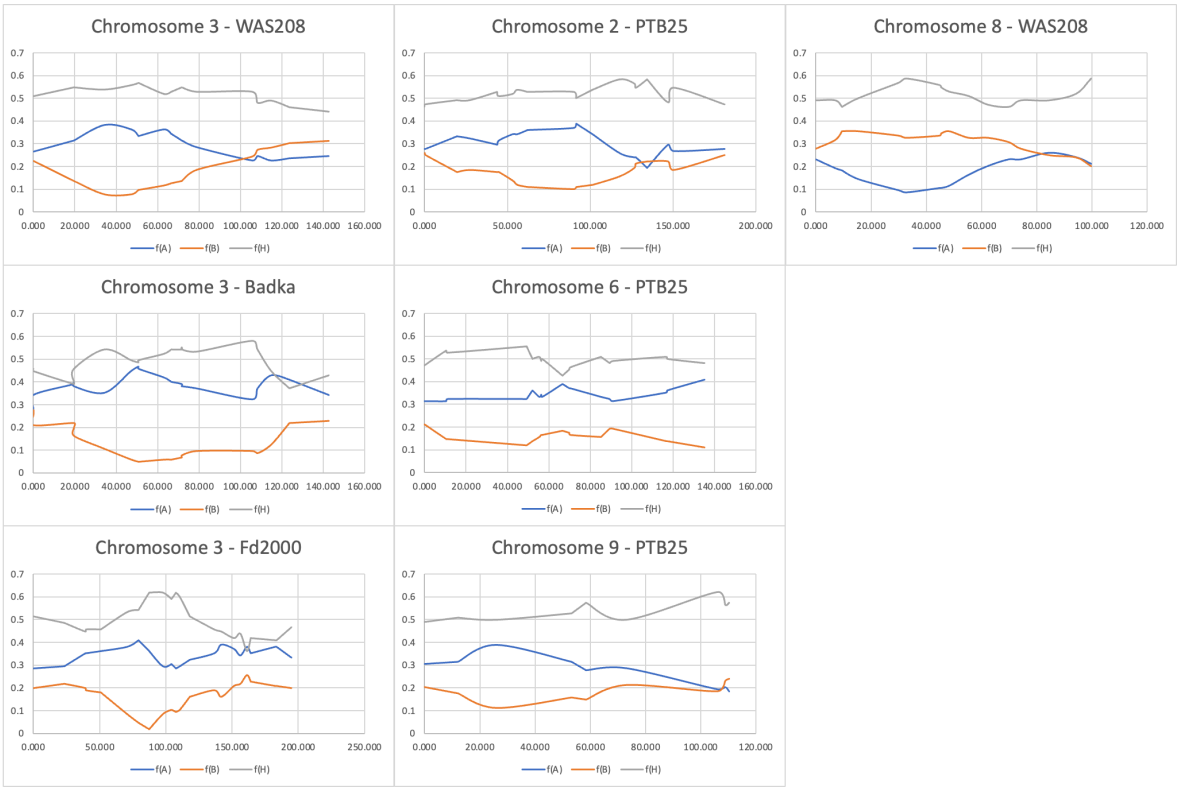

Figure S2 2-D plot for interaction analysis between genomic regions calculated in the FD2000 × BBT50 cross. A: RHBV incidence. B: RHBV severity

A

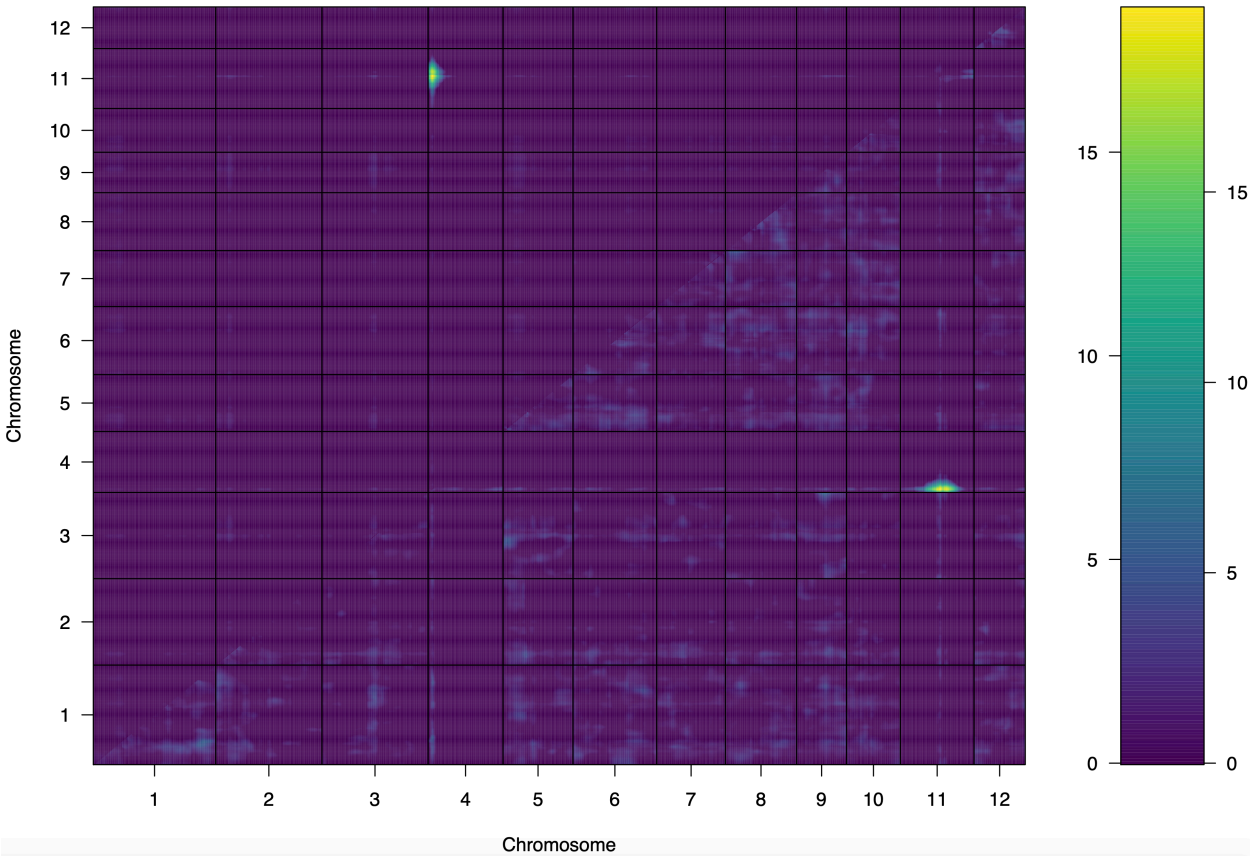

B

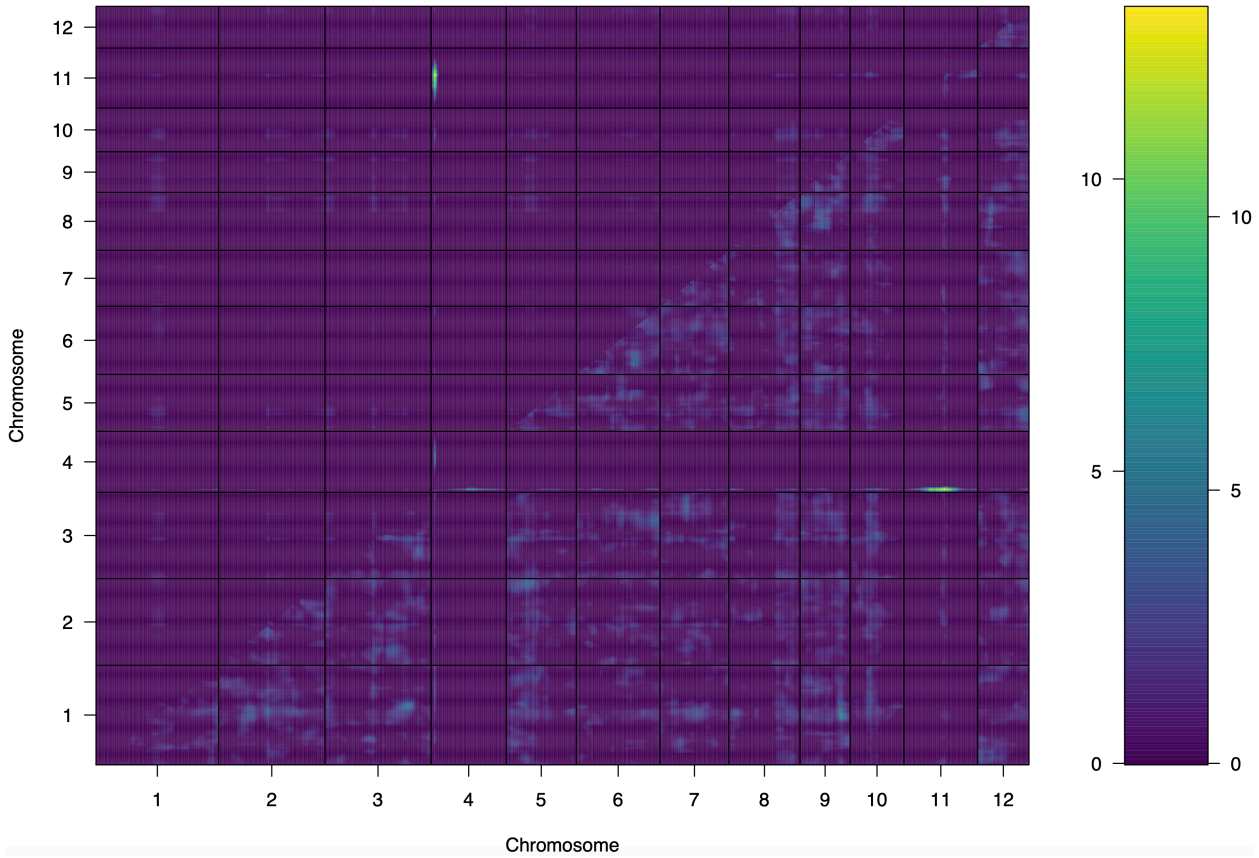

804 **Figure S3** Graphical genotyping showing probable local ancestry for the four RHB-resistant parents
805 (green arrows), in the two QTL regions *qHBV4.1* and *qHBV4.2* on chromosome 4. X-axis: physical
806 coordinates (in bp) along chromosome 4, spanning the region 2.6-4.4 Mbp. Y-axis: each row
807 represents a rice accession. Red: *indica* origin, including the Aus cluster. Blue: *japonica* origin,
808 including temperate, sub-tropical and tropical clusters. Gray: unclear origin. Local ancestry analysis
809 was performed using a set of SNP markers distributed along the whole rice genome and identified
810 previously in 97 diverse rice accessions (Duitama et al. 2015), using custom scripts. Briefly, the
811 accessions were first classified as *indica* or *japonica* by principal component analysis on the SNP set.
812 Then, the most frequent SNP haplotype (MFH) was searched in the *indica* and *japonica* groups using
813 adjacent windows of 224,000 bp (representing ~1 cM in rice). Finally, a simple matching similarity
814 index, SI, was calculated between each haplotype of each accession and the *indica* and *japonica*
815 MFHs. The *indica* or *japonica* origin of the haplotype was attributed if SI > 0.99.

816

817

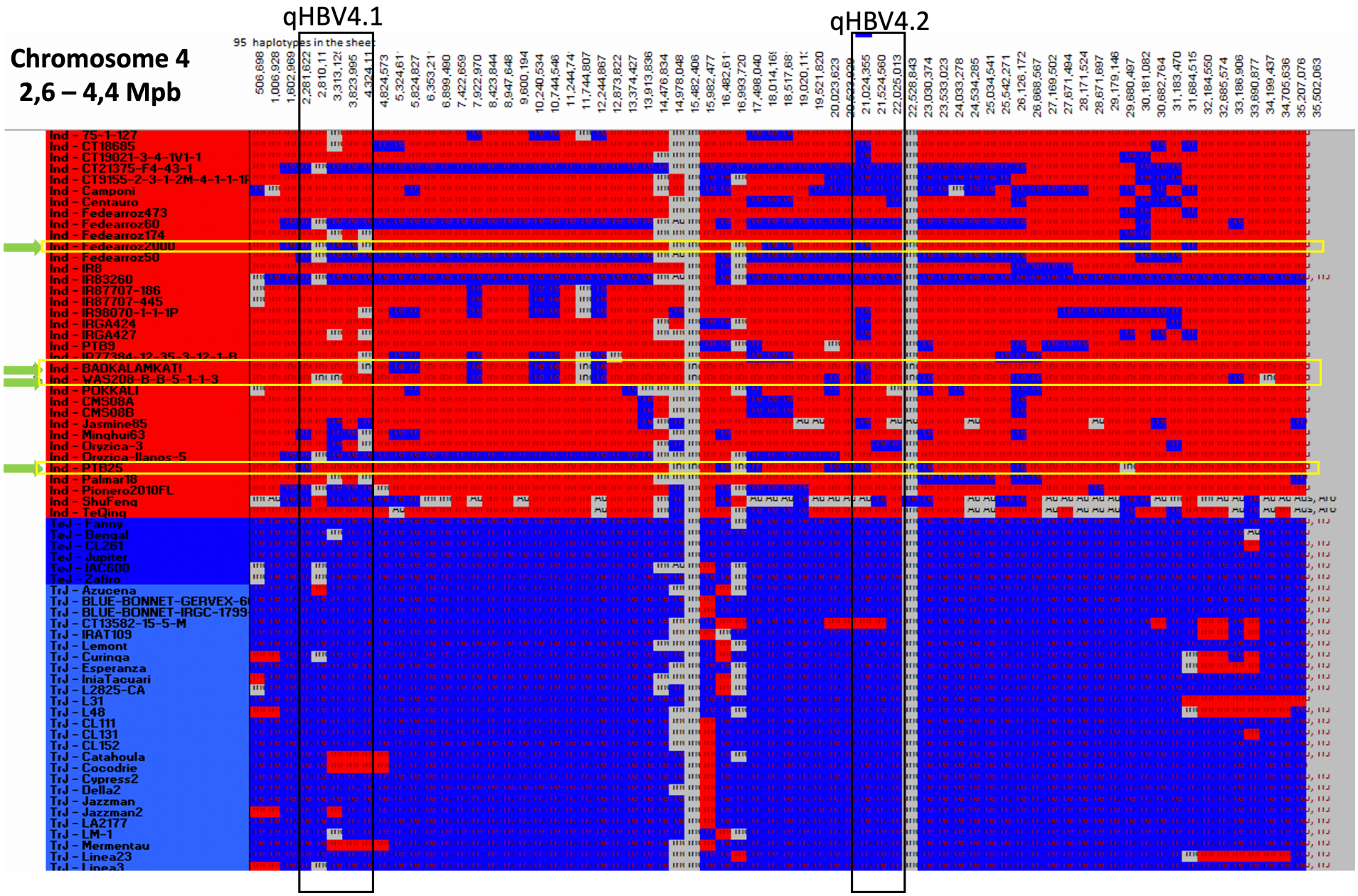
Chromosome 4
2,6 – 4,4 Mpb
qHBV4.1
qHBV4.2
95 haplotypes in the sheet
Ind - 75-1-127
Ind - CT18685
Ind - CT19021-3-4-1V1-1
Ind - CT21375-F4-43-1
Ind - CT9155-2-3-1-2M-4-1-1-1P
Ind - Camponi
Ind - Centauro
Ind - Fedearroz473
Ind - Fedearroz60
Ind - Fedearroz174
Ind - Fedearroz2000
Ind - Fedearroz50
Ind - IR8
Ind - IR83260
Ind - IR87707-186
Ind - IR87707-445
Ind - IR98070-1-1-1P
Ind - IRGA424
Ind - IRGA427
Ind - PTB9
Ind - BADKALAMKATI
Ind - WAS208-B-B-5-1-1-3
Ind - POKKALI
Ind - CMS08A
Ind - CMS08B
Ind - Jasmine85
Ind - Minghui63
Ind - Oryzica-3
Ind - Oryzica-llanos-5
Ind - PTB25
Ind - Palmar18
Ind - Pionero2010FL
Ind - ShuFeng
Ind - TeQing
TeJ - Fanny
TeJ - Bengal
TeJ - CL261
TeJ - Jupiter
TeJ - IAC600
TeJ - Zafiro
TrJ - Azucena
TrJ - BLUE-BONNET-GERVEX-6
TrJ - BLUE-BONNET-IRGC-1793
TrJ - CT13582-15-5-M
TrJ - IRAT109
TrJ - Lemont
TrJ - Curinga
TrJ - Esperanza
TrJ - IniaTacuari
TrJ - L2825-CA
TrJ - L31
TrJ - L48
TrJ - CL111
TrJ - CL131
TrJ - CL152
TrJ - Catahoula
TrJ - Cocodrie
TrJ - Cypress2
TrJ - Della2
TrJ - Jazzman
TrJ - Jazzman2
TrJ - LA2177
TrJ - LM-1
TrJ - Mermentau
TrJ - Linea23
TrJ - Linea3